

AD A093044

LEVEL II

12

DNA 5338T

COHERENCE BANDWIDTH LOSS IN TRANSIONOSPHERIC RADIO PROPAGATION

C. L. Rino

V. H. Gonzalez

A. R. Hessing

SRI International
333 Ravenswood Avenue
Menlo Park, California 94025

DTIC
ELECTRONIC
S DEC 11 1980
E

21 April 1980

Topical Report 2 for Period 4 January 1980–31 March 1980

CONTRACT No. DNA 001-80-C-0077

APPROVED FOR PUBLIC RELEASE;
DISTRIBUTION UNLIMITED.

THIS WORK SPONSORED BY THE DEFENSE NUCLEAR AGENCY
UNDER RDT&E RMSS CODE B322080462 I25AAXHX64017 H2590D.

Prepared for
Director
DEFENSE NUCLEAR AGENCY
Washington, D. C. 20305

DC FILE COPY

80 12 10 04

Destroy this report when it is no longer
needed. Do not return to sender.

PLEASE NOTIFY THE DEFENSE NUCLEAR AGENCY,
ATTN: STTI, WASHINGTON, D.C. 20305, IF
YOUR ADDRESS IS INCORRECT, IF YOU WISH TO
BE DELETED FROM THE DISTRIBUTION LIST, OR
IF THE ADDRESSEE IS NO LONGER EMPLOYED BY
YOUR ORGANIZATION.



UNCLASSIFIED

SECURITY CLASSIFICATION OF THIS PAGE (When Data Entered)

19 REPORT DOCUMENTATION PAGE		READ INSTRUCTIONS BEFORE COMPLETING FORM	
1. REPORT NUMBER DNA 5338T	2. GOVT ACCESSION NO. AD-4093044	3. RECIPIENT'S CATALOG NUMBER no.	
4. TITLE (and Subtitle) COHERENCE BANDWIDTH LOSS IN TRANSIONOSPHERIC RADIO PROPAGATION		5. FUNDING NUMBERS Topical Report, 2, for Period 4 Jan - 31 Mar 80	
6. AUTHOR(s) Charles L. Rino Victor H. Gonzalez Anne R. Hessing		7. PERFORMING ORG. REPORT NUMBER SRI Project 1284	
8. PERFORMING ORGANIZATION NAME AND ADDRESS SRI International 333 Ravenswood Avenue Menlo Park, California 94025		9. CONTRACT OR GRANT NUMBER(s) DNA 001-80-C-0077 ✓	
10. CONTROLLING OFFICE NAME AND ADDRESS Director Defense Nuclear Agency Washington, D.C. 20305		11. PROGRAM ELEMENT, PROJECT, TASK AREA & WORK UNIT NUMBERS Subtask I25AAXHX640-17	
12. MONITORING AGENCY NAME & ADDRESS (if different from Controlling Office) C. I. H.		13. REPORT DATE 21 Apr 1980	
		14. NUMBER OF PAGES 42	
		15. SECURITY CLASS (of this report) UNCLASSIFIED	
		15a. DECLASSIFICATION DOWNGRADING SCHEDULE	
16. DISTRIBUTION STATEMENT (of this Report) Approved for public release; distribution unlimited.			
17. DISTRIBUTION STATEMENT (of the abstract entered in Block 20, if different from Report)			
18. SUPPLEMENTARY NOTES This work sponsored by the Defense Nuclear Agency under RDT&E RMSS Code B322080462 I25AAXHX64017 H2590D.			
19. KEY WORDS (Continue on reverse side if necessary and identify by block number) Scintillation Power law Frequency coherence			
20. ABSTRACT (Continue on reverse side if necessary and identify by block number) In this report a theoretical model is developed that predicts the single-point, two-frequency coherence function for transionospheric radio waves. The theoretical model is compared to measured complex frequency correlation coefficients using data from the seven equispaced, phase-coherent UHF signals transmitted by the Wideband satellite. The theory and data are in excellent agreement. The theory is critically dependent upon → next page			

DD FORM 1 JAN 73 1473 EDITION OF 1 NOV 65 IS OBSOLETE

UNCLASSIFIED

SECURITY CLASSIFICATION OF THIS PAGE (When Data Entered)

4/10281

UNCLASSIFIED

SECURITY CLASSIFICATION OF THIS PAGE(When Data Entered)

conts 20. ABSTRACT (Continued)

the power-law index, and the frequency coherence data clearly favor the comparatively small spectral indices that have been consistently measured from the Wideband satellite phase data.

→ A model for estimating the pulse delay jitter induced by the coherence bandwidth loss is also developed and compared with the actual delay jitter observed on synthesized pulses obtained from the Wideband UHF comb. The results are in good agreement with the theory. The results presented in this report, which are based on an asymptotic theory, are compared with the more commonly used quadratic theory.

→ The model developed and validated in this report can be used to predict the effects of coherence bandwidth loss in disturbed nuclear environments. Simple formulas for the resultant pulse delay jitter are derived that can be used in predictive codes.

↖

UNCLASSIFIED

SECURITY CLASSIFICATION OF THIS PAGE(When Data Entered)

TABLE OF CONTENTS

SECTION	PAGE
LIST OF ILLUSTRATIONS	2
I INTRODUCTION	3
II THE SINGLE-POINT, TWO-FREQUENCY COHERENCE FUNCTION . .	6
III DATA ANALYSIS	12
IV EXCESS DELAY JITTER AND PULSE DISPERSION	18
V DISCUSSION	23
REFERENCES	26
APPENDIX--APPROXIMATION TO THE PHASE STRUCTURE FUNCTION	29

Accession For	
NTIS GRA&I	<input checked="" type="checkbox"/>
DDC TAB	<input type="checkbox"/>
Unannounced	<input type="checkbox"/>
Justification	<input type="checkbox"/>
By _____	
Distribution/ _____	
Availability Codes	
Dist	Available and/or special
A	

LIST OF ILLUSTRATIONS

FIGURE		PAGE
1	Measured Single-Point Two-Frequency Correlation Functions from Kwajalein Data Plotted Against H as Derived from Simultaneous L-Band S_4 Data	14
2	Measured Single-Point Two-Frequency Correlation Functions from Ancon Data Plotted Against H as Derived from Simultaneous L-Band S_4 Data	15
3	Comparison of Measured Complex Frequency Decorrelation and Theoretical Predictions from Phase Screen Theory.	17
4	Synthesized Pulses from Wideband Satellite Data Showing Effects of Coherent Bandwidth Loss	21
5	Measurements of Delay Jitter from Synthesized Pulses Using Wideband Satellite Data Together with Theoretical Prediction from Eq. (IV-4)	22
6	Theoretical Calculations of Delay Jitter Caused by Loss of Coherence Bandwidth.	25
A-1	Plot of Normalized Structure Function Showing Dependence on Spectral Slope	30
A-2	Plot of Small q_0 Approximation to Phase Structure Function (valid for $v < 1.5$) Superimposed on Exact Curves	32
A-3	Plot of Quadratic Approximation to Phase Structure Function Superimposed on Exact Curves.	33

I INTRODUCTION

The dispersive nature of the ionosphere causes a systematic time delay of radio signals that propagate through it. Depending on the precision required, this time delay can be compensated by using ionospheric models (Klobuchar, 1975) or dual-frequency transmissions (see for example, Spilker, 1978). Under disturbed conditions there is a random "excess" delay that cannot be compensated and a distortion of the transmitted waveform. Such effects are a concern in precision navigation systems such as the Global Positioning System (GPS).

The phenomenon is common to the propagation of laser pulses in turbulent media (Liu and Yeh, 1980) and radiowaves in the interplanetary medium (Woo, 1975). Yeh and Liu (1977a,b; 1979) and Liu and Yeh (1979) have developed a detailed theory for computing the excess delay and waveform distortion. There are, however, few data sets against which the various theoretical predictions can be tested.

In this report we have developed a theoretical formulation of the coherence bandwidth problem (see Section II) that differs from Yeh and Liu's method in that (1) it fully accommodates angle effects in anisotropic media, (2) it gives an explicit formula for the single-point, two-frequency coherence function, and (3) it uses asymptotic rather than Taylor series expansions, thereby preserving the dependence on the power-law index. We also note that our results do not depend on the precise value of the outer- or inner-scale cutoff wavenumbers.

To validate the theoretical predictions (Section III), we have used data from the Wideband satellite, which transmits phase-coherent signals at S-band, L-band, UHF, and VHF. The UHF signal is a comb of seven equally spaced frequencies ($413.02 \pm n11.47$ MHz, where $n = 0, 1, 2, 3$) that was uniquely designed for coherence bandwidth measurements. Indeed, the name "Wideband satellite" was coined because of this capability. [See Fremouw et al. (1978) for a detailed description of the experiment.]

The theory and experimental data are in excellent agreement. As in the theory of the time structure of intensity scintillation under strong scatter conditions (Rino and Owen, 1980), a single parameter characterizes the combined effects of changing perturbation strength and propagation distance. The effect of a more shallowly sloped spectral density function is to produce more frequency decorrelation for a fixed perturbation level. This is clearly evident in the data.

The comparisons of measured and predicted frequency coherence functions validate the theory, but they do not immediately relate to observable system effects such as delay jitter or pulse distortion. Thus, we have used the seven coherent signals from the Wideband satellite to synthesize disturbed pulses and then measure the actual delay jitter (Section IV). The results are in good agreement with theoretical calculations based on the single-point, two-frequency coherence function derived in Section II.

To introduce the principal quantity of interest, we recall that the ionosphere is a linear but time-varying transmission medium. Thus, it can be characterized by a time-varying transfer function $h(t;f)$ (Bello, 1963). If a signal

$$S(t) = \text{Re}[v(t) \exp \{2\pi i f_c t\}] \quad (\text{I-1})$$

is transmitted, the received signal, $S_o(t)$, admits a similar representation with $v(t)$ replaced by

$$v_o(t) = \int_{-\infty}^{\infty} \hat{v}(f) h(t; f + f_c) \exp \{2\pi i f t\} df \quad (\text{I-2})$$

where $\hat{v}(f)$ is the Fourier transform of $v(t)$. One assumes that $\hat{v}(f) \cong 0$ for $|f| > F/2$, and that $F \ll f_c$.

An incoherent receiver effectively measures $\langle |v_o(t)|^2 \rangle$. By direct computation from Eq. (I-2) it can be shown that

$$\langle |v_o(t)|^2 \rangle = \iint \hat{v}(f+\delta f/2) \hat{v}^*(f-\delta f/2) \langle h(t;f_c+t-\delta f/2) h^*(t;f_c+f-\delta f/2) \rangle \\ \times \exp \{2\pi i \delta f t\} d\delta f df \quad . \quad (I-3)$$

Thus, the entity that characterizes the randomly dispersive effects of the transionospheric channel is the single-point, two-frequency correlation function

$$R(\delta f;f) = \langle h(t;f+\delta f/2) h^*(t;f-\delta f/2) \rangle \quad . \quad (I-4)$$

If coherent detection is used, a similar expression for the power at the output of a correlator followed by a low-pass filter can be derived, provided that $h(t;f)$ is essentially constant over intervals of duration $1/F$. This is generally a very good assumption. Thus, the ionosphere-induced delay jitter should not be significantly different for coherent or noncoherent detection.

II THE SINGLE-POINT, TWO-FREQUENCY COHERENCE FUNCTION

Following Fante (1978), we first consider a freely propagating wavefield $u(\vec{\rho}_\perp, z_\ell; f_1)$ that subtends only a narrow range of scattering angles. If we take $z_\ell = 0$ as a reference plane and apply the Huygens-Fresnel principle,

$$u(\vec{\rho}_\perp, z_\ell; f_1) = \frac{k_1}{2\pi i z_\ell} \iint \exp \left\{ -i \xi^2 \frac{k_1}{2z_\ell} \right\} u(\vec{\rho}_\perp + \vec{\xi}, 0; f_1) d\vec{\xi} \quad (\text{II-1})$$

where $k = 2\pi/\lambda = 2\pi f/c$. The subscripts ℓ and \perp denote coordinates along and transverse to the propagation direction, respectively. Since we are only interested in a single-point correlation function, there is no need to use the general formulation developed in Rino and Fremouw (1977).

Assuming "frozen" irregularity structures (the Taylor hypothesis), it follows that $h(t; f_1) = u(\vec{v}_\perp t, z_\ell; f_1)$. Thus, by substituting Eq. (II-1) into Eq. (I-4), we have

$$\begin{aligned} & \langle h(t; f_1) h^*(t; f_2) \rangle \\ &= \frac{k_1 k_2}{(2\pi z_\ell)^2} \iiint \exp \left\{ -i \left[\xi^2 \frac{k_1}{2z_\ell} - \xi'^2 \frac{k_2}{2z_\ell} \right] \right\} R_u(\Delta \vec{\xi}, f_1, f_2) d\vec{\xi} d\vec{\xi}' \end{aligned} \quad (\text{II-2})$$

where $R(\Delta \vec{\xi}, f_1, f_2)$ is the two-frequency spatial coherence function of $u(\rho_\perp, 0; f)$. We have assumed that u is spatially homogeneous. This assumption does not, however, require homogeneous phase variations. By changing the integration variables in Eq. (II-2) to $\Delta \vec{\xi}' = \vec{\xi}' - \vec{\xi}$ and $\vec{\chi} = (\vec{\xi} + \vec{\xi}')/2$, we can isolate and evaluate the integral over $\vec{\chi}$. After a series of algebraic manipulations, Eq. (II-2) can then be put in the form

$$\langle h(t; f_1) h^*(t; f_2) \rangle$$

$$= \frac{1}{2\pi i} \frac{k_1 k_2}{(k_1 - k_2) z_\ell} \iint \exp \left\{ i \frac{\Delta \vec{\xi}^2}{2} \frac{k_1 k_2}{(k_1 - k_2) z_\ell} \right\} R_u(\Delta \vec{\xi}; f_1, f_2) d\Delta \vec{\xi} \quad (II-3)$$

Equation (II-3) is a completely general expression for the free-space propagation of the two-frequency coherence function. To evaluate $R_u(\Delta \vec{\xi}; f_1, f_2)$, the Rytov approximation can be applied, as was done by Ishimaru (1972) and Fante (1978). It is, of course, simpler to use an equivalent phase-screen whereby all diffraction effects develop in free space. Because the results based on the equivalent phase screen model seem to preserve all essential aspects of the scintillation phenomenon, we have used that model herein.

To apply the phase screen model we let

$$u(\vec{\xi}; 0; f_1) = \exp \{ i r_e \lambda \Delta N_\ell(\vec{s}) \} \quad (II-4)$$

where $\Delta N_\ell(\vec{\xi})$ is the perturbation to the integrated electron content. If $\Delta N_\ell(\vec{\xi})$ is gaussian, it is readily shown from Eq. (II-4) that

$$R_u(\Delta \vec{\xi}; f_1, f_2) = \exp \left\{ -r_e^2 \frac{\lambda^2}{1 - \epsilon^2} D_{\Delta N_\ell}(\Delta \vec{\xi}) - r_e^2 \lambda^2 \frac{2\epsilon^2}{1 - \epsilon^2} \langle \Delta N_\ell^2 \rangle \right\} \quad (II-5)$$

where

$$f = c/\lambda = (f_1 + f_2)/2 \quad (II-6a)$$

$$\delta f = f_2 - f_1 \quad (II-6b)$$

$$\epsilon = \delta f / (2f) \quad (II-6c)$$

and $D_{\Delta N_\ell}(\Delta \vec{\xi}) = \langle (\Delta N_\ell(\vec{\xi}) - \Delta N_\ell(\vec{\xi}'))^2 \rangle$ is the structure function for $\Delta N_\ell(\vec{\xi})$. The gaussian assumption should be regarded as a sufficient but not strictly necessary condition (Rino, 1979b).

If $\epsilon \ll 1$, then Eq. (II-5) simplifies to

$$R_u(\Delta \vec{\xi}; f, \delta f) = \exp \{ -D_{\delta \phi}(\Delta \vec{\xi}) \} \exp \{ -2\epsilon^2 \sigma_{\delta \phi}^2 \} \quad (II-7)$$

where $\sigma_{\delta\phi}^2$ is the phase variance, and $D_{\delta\phi}(\vec{\Delta\xi})$ is the phase structure function. Hereafter, it is understood that any quantity that depends implicitly on frequency is to be evaluated at the mean frequency, Eq. (II-6a). Note, however, that the mean frequency f need not equal f_c .

By similarly approximating $(k_1 k_2)/(k_1 - k_2)$, changing variables in Eq. (II-3), and substituting from Eq. (II-7) we obtain the general result

$$R(\delta f; f) = \frac{i}{2\pi} \iint \exp \{-i \Delta\xi^2/2\} \exp \{-D_{\delta\phi}(\vec{\Delta\xi} [2Z \delta f/f]^{1/2})\} d\vec{\Delta\xi} \\ \times \exp \{-\sigma_{\delta\phi}^2 2\epsilon^2\} \quad (II-8)$$

Since we are working in a transverse coordinate system, $D_{\delta\phi}(\vec{\Delta\xi})$ is functionally dependent on the quadratic form

$$y^2 = \frac{C' \Delta\xi_z^2 - B' \Delta\xi_x \Delta\xi_y + A' \Delta\xi_y^2}{A' C' - B'^2/4} \quad (II-9)$$

where A' , B' , and C' are defined by Eqs. (26a), (26b), and (26c) in Rino (1979a).

By first rotating variables to remove the $\Delta\xi_x \Delta\xi_y$ term and then performing a series of variable changes, it is possible to reduce Eq. (II-8) to the single integral

$$R(\delta f; f) = i \sqrt{\beta^2 - \alpha^2} \int_0^\infty J_0(\omega\alpha) \exp \{-i\omega\beta\} \\ \times \exp \{-D_{\delta\phi}([\omega 2Z \delta f/f]^{1/2})\} d\omega \exp \{-\sigma_{\delta\phi}^2 2\epsilon^2\} \quad (II-10)$$

where

$$A'' = \frac{1}{2}(A' + C' + D') \quad (II-11a)$$

$$C'' = \frac{1}{2}(A' + C' - D') \quad (II-11b)$$

$$D' = \sqrt{(A' - C')^2 + B'^2} \quad (\text{II-11c})$$

$$\alpha = (A'' - C'')/4 \quad (\text{II-11d})$$

$$\beta = (A'' + C'')/4 \quad (\text{II-11e})$$

The same transformation was used in Rino (1979a) [cf. Eqs. (29a), (29b), and (29c)]. For isotropic irregularities, $A'' = C'' = 1$, so that $\beta = 0.5$ and $\alpha = 0$. For highly anisotropic irregularities, $A'' \sim a^2$, where a is the axial ratio, and $C'' = 1$. For large a , $\alpha \sim \beta$, although $\beta^2 - \alpha^2 \equiv A''C''/4 \sim a^2/4$.

In a power-law environment the general form of the phase structure function is too cumbersome to be of practical value. Thus, approximations must be used that take advantage of the fact that the outer scale is typically much larger than the scale sizes that make a significant contribution to the signal over time intervals of interest. Two different approximations have been used.

For a three-dimensional spectral density function of the form

$$\Phi_{\Delta N_e}(q) = C_s q^{-(2\nu+1)} \quad (\text{II-12})$$

with $0.5 < \nu < 1.5$, it can be shown by asymptotic methods that

$$D_{\delta\phi}(y) \sim C_{\delta\phi}^2 |y|^{2\nu-1} \quad (\text{II-13})$$

where $C_{\delta\phi}^2$ is the phase structure constant,

$$C_{\delta\phi}^2 = \frac{C_p}{2\pi} \frac{2\Gamma(1.5-\nu)}{\Gamma(\nu+0.5)(2\nu-1)2^{2\nu-1}} \quad (\text{II-14})$$

In this model, which has been used extensively in neutral turbulence studies, the spectral density function and the structure function have complementary power-law forms. There is, moreover, no dependence on the inner- or outer-scale cutoff wavenumbers.

Alternatively, one may use a Taylor series expansion of $D_{\delta\phi}(y)$ and retain only the quadratic term. In that case,

$$D_{\delta\phi}(y) \sim 2\sigma_{\delta\phi}^2 D_1(q_0 y)^2 \quad (\text{II-15})$$

where the form of D_1 is given in the Appendix. Comparisons of the quadratic and asymptotic approximations are also given in the Appendix. The quadratic approximation is strictly valid only for steeply sloped spectral density functions such that $\nu > 1.5$. It should be noted that both $\sigma_{\delta\phi}^2$ and D_1 depend on the outer-scale wavenumber q_0 , and D_1 depends on the inner-scale cutoff wavenumber as well.

If Eq. (II-13) is substituted into Eq. (II-10) the result is

$$\begin{aligned} R(\delta f; f) = & 2\sqrt{\beta^2 - \alpha^2} \int_0^\infty J_0(\omega\alpha) \exp\{-i\omega\beta\} \\ & \times \exp\left\{-H\left|\frac{\delta f}{f}\right|^{\nu-0.5} \omega^{\nu-0.5}\right\} d\omega \exp\{-\sigma_{\delta\phi}^2 2\epsilon^2\} \end{aligned} \quad (\text{II-16})$$

where

$$H = G C_{\delta\phi}^2 |2Z|^{\nu-0.5} . \quad (\text{II-17})$$

The factor G accounts for anisotropic media. It is defined and discussed in detail in Rino (1979a,b). The quadratic approximation gives rise to a similar form with the exception that $\nu-0.5$ is replaced by unity in Eqs. (II-16) and (II-17), and $C_{\delta\phi}^2$ in Eq. (II-17) is replaced by $2\sigma_{\delta\phi}^2 D_1 q_0^2$.

Unfortunately, Eq. (II-16) cannot be analytically evaluated for ν within the admissible range $0.5 > \nu > 1.5$. However, following Fante (1978), who encountered a similar integral in this context, one can replace the $\nu-0.5$ term in Eqs. (II-16) and (II-17) by unity. The integral can then be evaluated analytically, giving the result

$$R(\delta f; f) \cong \frac{\sqrt{\beta^2 - \alpha^2} \exp \{-\sigma_{\phi}^2 2\epsilon^2\}}{\sqrt{\left(\beta - iH \left| \frac{\delta f}{f} \right| \right)^2 - \alpha^2}} . \quad (\text{II-18})$$

We shall see that Eq. (II-18) predicts a correlation level that is too high for a given value of H . Under the quadratic approximation, however, Eq. (II-18) is exact.

In effect, Eq. (II-18) becomes a better and better approximation as the spectral index parameter approaches $\nu = 1.5$. For more steeply sloped spectra, one expects the quadratic approximation to give accurate results. The crucial factor, therefore, is the spectral index. We shall see in Section III that the data clearly fall below the predictions of Eq. (II-18), thereby further supporting the more shallowly sloped spectral density functions that have now been verified by a number of different studies (Rino, 1979a,b; Rino and Owen, 1980).

III DATA ANALYSIS

As noted in the Introduction, the Wideband satellite transmits seven equispaced, phase-coherent signals at UHF. Thus, 21 values of $\langle u(f_1)u^*(f_2) \rangle$ can be measured with different values of f_1 and f_2 . It is convenient, however, to use only the three symmetric frequency pairs about 413.0244 MHz. In that case the mean frequency $f = (f_1 + f_2)/2$ is invariant and identically equal to the center frequency. The corresponding values of $\delta f/f$ are 0.056, 0.111, and 0.167.

To obtain a data base of highly disturbed passes we have used the same equatorial Wideband passes as were processed and analyzed in Rino and Owen (1980). The seven UHF channels were detrended with a 10-s detrend filter cutoff at a 100-Hz sample rate. For single-time-point measurements the sample rate is not critical. Thus, to save computer time the lower data rate was used. The 28 complex correlation coefficients were then computed and recorded for further processing.

Now, from Eqs. (II-16) and (II-17) we see that $R(\delta f; f)$ depends on the propagation geometry through the α and β terms as well as H . However, for the highly elongated irregularities near the geomagnetic equator we can use the limiting values $\alpha \sim (a^2 + 1)/4$, $\beta \sim (a^2 - 1)/4$, and $\beta^2 - \alpha^2 \sim a^2/4$, where a is the axial ratio. Thus, the principal variable in Eq. (II-16) is the combined perturbation strength and propagation distance parameter, H .

We also note that Eq. (II-16) admits a weak dependence on the rms phase, $\sigma_{\delta\phi}$. Since the value of the rms phase itself depends on the interval over which it is measured, $R(\delta f; f)$ will exhibit a similar non-stationary behavior. From Eq. (II-5) it can be seen that the phase term is a remnant of the purely dispersive behavior of the ionosphere. Its contribution is generally small, and in any case is readily computed because we measure $\sigma_{\delta\phi}$. Alternatively, one can remove linear phase trends across the UHF comb before the correlation coefficients are computed.

The parameter H depends on the geometrical enhancement factor, G , the phase structure constant, $C_{\delta\phi}$, and the Fresnel parameter, Z . Since the phase turbulent strength, T , can be measured, and $T \propto GC_{\delta\phi}^2 v_{\text{eff}}^{2\nu-1}$ [see Rino (1977), Eq. (18)], we could determine $GC_{\delta\phi}^2$ by first estimating the effective scan velocity v_{eff} . The problem is that v_{eff} depends on both the assumed layer height and the propagation geometry as does Z . If this approach were pursued, therefore, the data sorting would depend on an unknown parameter--namely, the height of the equivalent phase screen.

We note, however, that under conditions of weak scatter for S_4 ,

$$S_4^2 = C_P Z^{\nu-1/2} \left[\frac{\Gamma(2.5-\nu)/2}{2\sqrt{\pi} \Gamma(\nu+0.5)/2 (\nu-0.5)} \right] \mathcal{J} \quad (\text{III-1})$$

where $\mathcal{J} \sim \Gamma(\nu)/[\sqrt{\pi} \Gamma(\nu+1/2)]$ for large ν (Rino, 1979a). Since $G \sim 1$ under the same conditions, H and S_4^2 are simply proportional. The proportionality constant depends on ν but is readily calculated by comparing Eqs. (II-14), (II-17), and (III-1). In our data analysis we used the measured L-band S_4 scintillation index, which was generally in the weak scatter regime ($S_4 \leq 0.6$), to compute H for an assumed value of ν .

In Figure 1, measured values of $R(\delta f; f)$ plotted against H are shown for a set of disturbed passes recorded at Kwajalein. The numbers above each data point indicate the number of measured $R(\delta t; t)$ values that fell in the particular H bin. The error bars indicate the maximum excursion for the measured standard deviation of the $\Delta f/f = 0.056$ data points, and the minimum excursion for the corresponding deviation of the $\Delta f/f = 0.167$ data points. In Figure 2 similar measurements for the Ancon data are shown.

Both data sets show that measured values of $R(\Delta f; f)$ are well ordered by the H parameter. The exact value of H depends on the ν value and weakly on the propagation geometry. The particular value $\nu = 1.5$, which corresponds to a one-dimensional phase spectral index of 2.5, is a representative median value from spectral analysis of the corresponding phase data (Rino, 1979a; Rino and Owen, 1980).

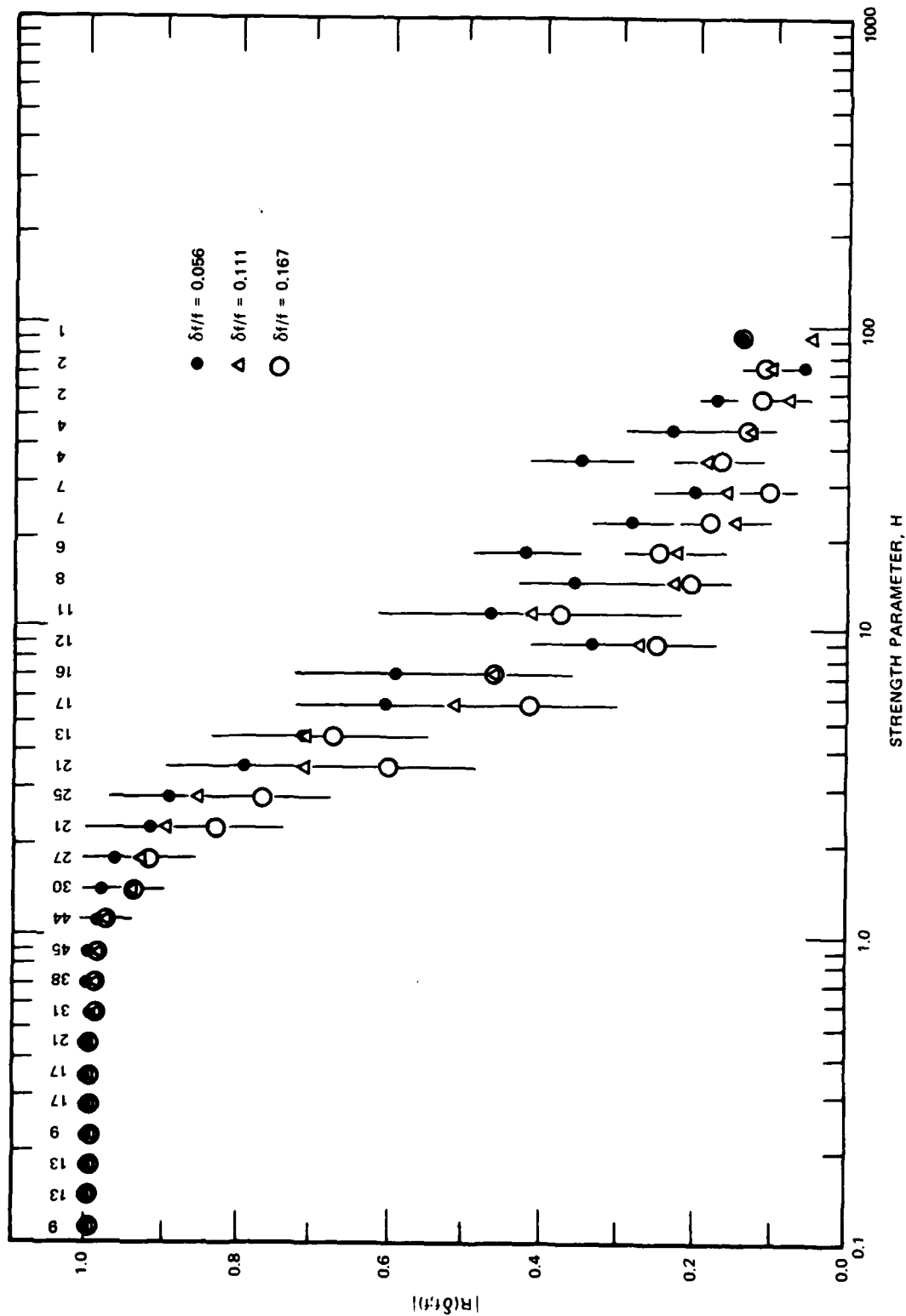


FIGURE 1 MEASURED SINGLE-POINT TWO-FREQUENCY CORRELATION FUNCTIONS FROM KWAJALEIN DATA PLOTTED AGAINST H AS DERIVED FROM SIMULTANEOUS L-BAND S_4 DATA

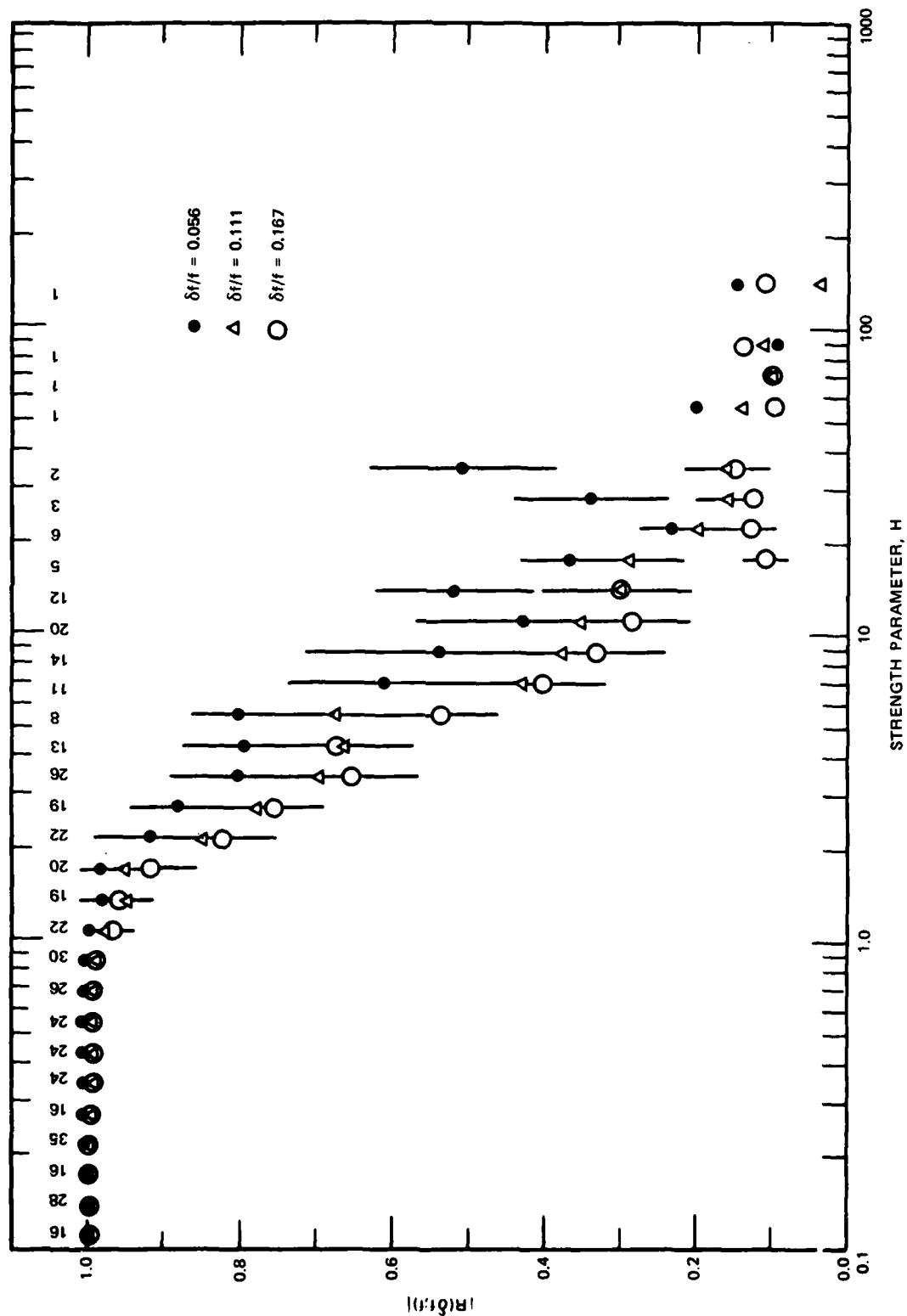


FIGURE 2 MEASURED SINGLE-POINT TWO-FREQUENCY CORRELATION FUNCTION FROM ANCON DATA PLOTTED AGAINST H DERIVED FROM SIMULTANEOUS L-BAND S_4 DATA

To compare the measured $R(\delta f; f)$ values with the theory, we have numerically integrated Eq. (II-16) with $\alpha = (a^2 + 1)/4$, and $\beta = (a^2 - 1)/4$, and different values of ν . Only $\Delta f/f = 0.167$ was used because it gives the maximum decorrelation for a given value of H , and the integral is most easily evaluated in such regimes. In Figure 3 the theoretical results are plotted together with the approximate formula Eq. (II-18). Also shown in the figure are measured values of $R(\delta f; f)$ from the Ancon data.

We first note that the approximate formula, Eq. (II-18), always predicts a smaller frequency decorrelation than the exact formula, and that the amount of decorrelation for a given value of H increases with decreasing ν . The actual data values systematically fall below the theoretical curves for decreasing ν values as H increases. This behavior suggests a variable spectral index, which has indeed been observed and used to improve the theoretical fit to intensity coherence measurements under strong scatter conditions (Rino and Owen, 1980). The spectral index decreases with increasing perturbation strength. Thus the theory and data are in excellent agreement.

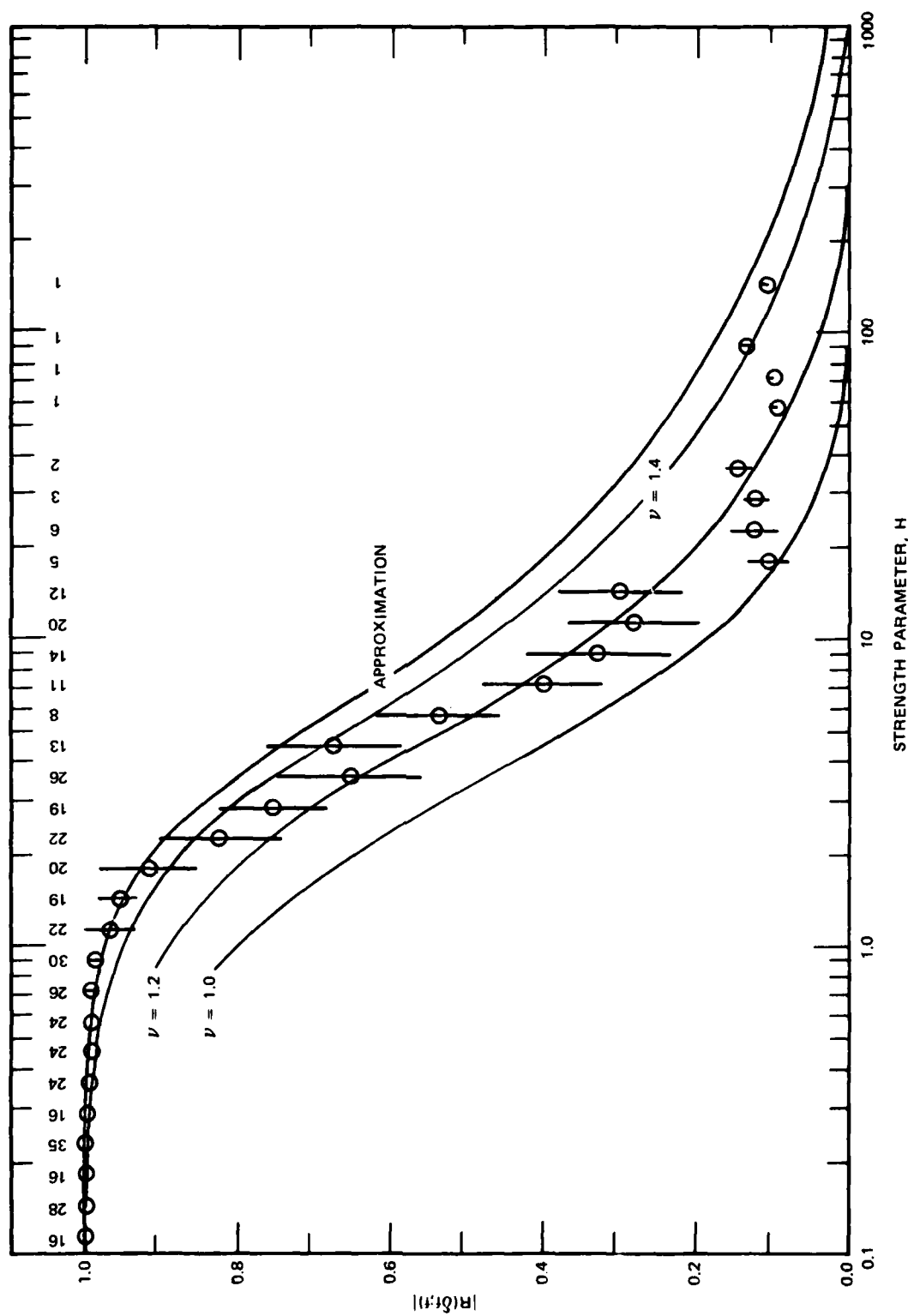


FIGURE 3 COMPARISON OF MEASURED COMPLEX FREQUENCY DECORRELATION AND THEORETICAL PREDICTIONS FROM PHASE SCREEN THEORY

IV EXCESS DELAY JITTER AND PULSE DISPERSION

We have developed a model that characterizes the single-point two-frequency coherence function and showed that it is in good agreement with data from the Wideband satellite. As yet, however, we have not developed a simple means of assessing the impact of the randomly dispersive effects on broadband waveforms. To this end, Yeh and Liu (1977a) have computed the temporal moments

$$M_n = \int_{-\infty}^{\infty} t_n \langle |v_o(t)|^2 \rangle dt \quad (IV-1)$$

They showed, for example, that if $\int tv(t)dt = 0$, then

$$\tau_d \triangleq M_1 = \frac{1}{2\pi i} \int_{-F/2}^{F/2} |\hat{v}(f)|^2 \left[\frac{\partial}{\partial \delta f} R(\delta f; \bar{f}) \right]_{\delta f=0} df \quad (IV-2)$$

and

$$\Omega \triangleq M_2 - \int t^2 |v(t)|^2 dt = \frac{1}{(2\pi i)^2} \int_{-F/2}^{F/2} |v(f)|^2 \left[\frac{\partial^2}{\partial \delta f^2} R(\delta f; \bar{f}) \right]_{\delta f=0} df. \quad (IV-3)$$

M_1 is a measure of the average delay jitter and Eq. (IV-3) measures the waveform spreading. However, from Eq. (II-10), the n^{th} derivative of $R(\delta f; f)$ is proportional to $|\delta f/f|^{\nu-(n+0.5)}$, which is singular at $\delta f = 0$ when $0.5 < \nu < 1.5$. This implies that in a power-law environment $\langle |v_o(t)|^2 \rangle$ develops a slowly decaying tail.

The effect is not an artifact of the model, but rather an indication that one cannot meaningfully evaluate Eq. (IV-1) over an arbitrarily large time interval. The singularity can, of course, be removed by introducing an inner-scale cutoff. We believe, however, that since an

inner-scale cutoff has not been detected in scintillation data, it is more realistic to use Eqs. (IF-2) and (IV-3) with the derivatives evaluated at $\delta f = \tau_c^{-1}$ instead of $\delta f = 0$ is on the order of the waveform duration.

It happens, however, that if the approximate form of Eq. (II-18) is used, the singularity is also removed. It is then readily shown that if $F \ll f_c$,

$$\tau_d \cong \frac{H}{2\pi f_c} \frac{\beta}{\beta^2 - \alpha^2} \quad (\text{IV-4})$$

and

$$\Omega_d \cong \left(\frac{H}{2\pi f_c} \right)^2 \frac{\beta^2 + \alpha^2}{(\beta^2 - \alpha^2)^2} \quad (\text{IV-5})$$

For isotropic irregularities at normal incidence, $\beta = 1$ and $\alpha = 0$. In that case, $\Omega_d = (\tau_d)^2$. The same relationship holds in a deterministically dispersive uniform ionosphere where $\tau_d \propto N_T/f^2$, and N_T is the integrated content.

It remains to show how good a measure Eq. (IV-4) or more refined estimates are, since they have practical ramifications. We first note from Eq. (I-2) that the modulation imparted on a sinusoidal transmission is $h(t;f)$. Thus, from the Wideband satellite UHF comb of seven frequencies we can synthesize a pulse as

$$v_o(\tau) = \sum_{k=-3}^3 h(t;f_k) \exp \{2\pi i k \Delta f \tau\} \quad (\text{IV-6})$$

where $f_k = 413.02 \pm k\Delta f$, and $\Delta f = 11.47$ MHz. For example, if there is no disturbance, so that $h(t;f_k) \cong 1$, then it is easily shown from Eq. (IV-6) that

$$|v_o(\tau)|^2 = \frac{\sin^2 [7\pi \Delta f \tau]}{\sin^2 [\pi \Delta f \tau]} \quad (\text{IV-7})$$

The pulse is, of course, non-causal and it has range ambiguities at multiples of $1/\Delta f = 0.0872 \mu s$. This is of no consequence for our purposes here, however, and we can use Eq. (IV-6) at different t values to first estimate $\langle |v_o(\tau)|^2 \rangle$ and then compute various signal moments as defined by Eq. (IV-1). Because the procedure is somewhat time consuming, only the first moment was actually computed.

A typical set of $\langle |v_o(\tau)|^2 \rangle$ estimates is shown in Figure 4. The pulses were averaged over a 20-s data interval. The numbers on the right-hand edge of each pulse estimate give the corresponding H value. For $H \geq 3$, the pulses show severe distortion as we should expect from the data in Figures 1 and 2.

Estimates of the first moments together with the theoretical prediction of τ_d from Eq. (IV-4) are shown in Figure 5. There is a large amount of scatter in the data because of the sensitivity of simple moment estimates to small fluctuations at large t values, which is the nature of ionospheric coherence bandwidth effects. In any case, the crude theoretical calculations upon which Eq. (IV-4) is based seem to give an acceptable result for engineering purposes. There is a tendency for the actual delay jitter to be larger than the predicted value from Eq. (IV-4). This is expected since the observed decorrelation is always somewhat greater than that predicted by Eq. (II-18) from which Eq. (IV-4) was derived.

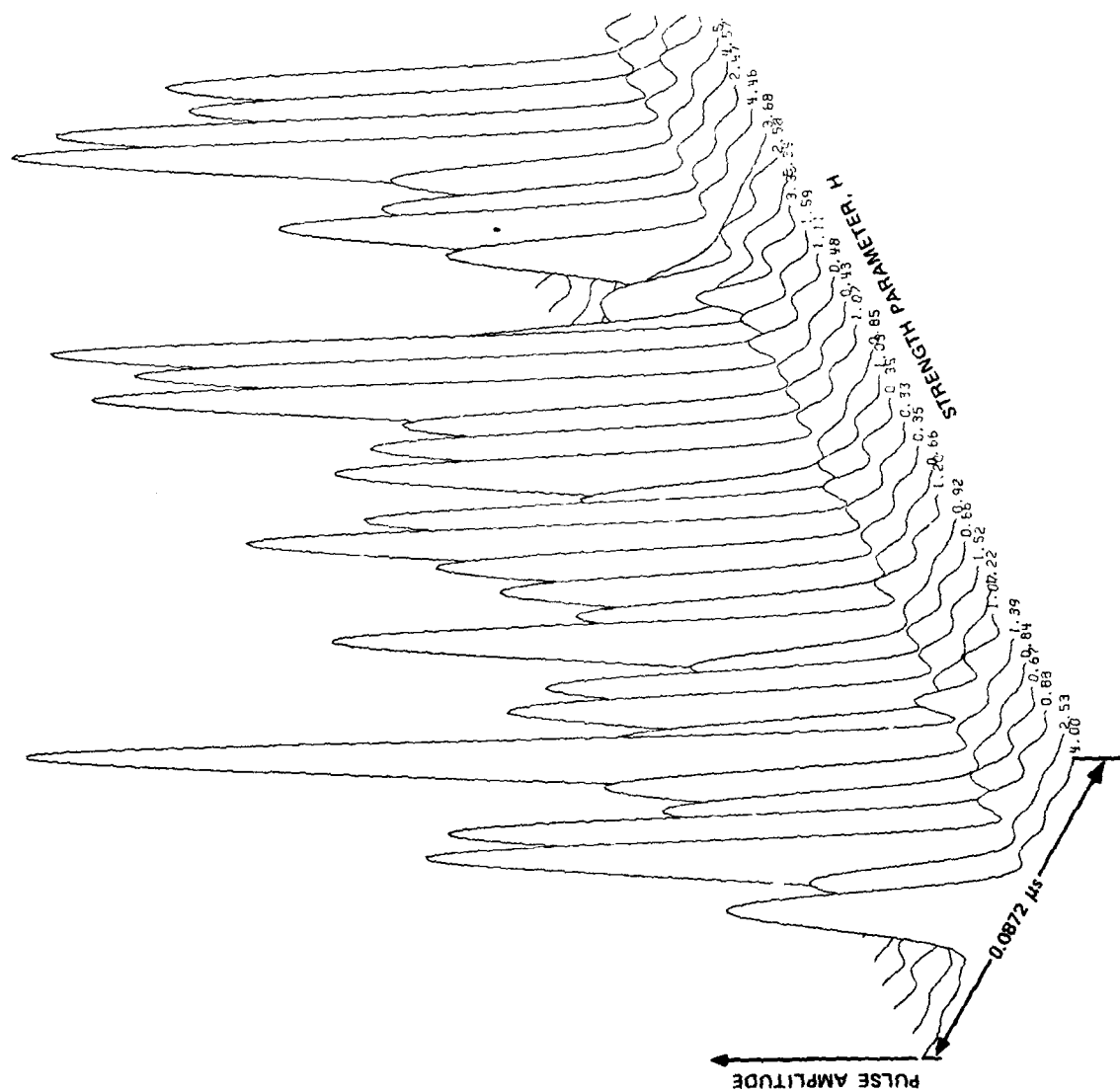


FIGURE 4 SYNTHESIZED PULSES FROM WIDEBAND SATELLITE DATA SHOWING EFFECTS OF COHERENT BANDWIDTH LOSS

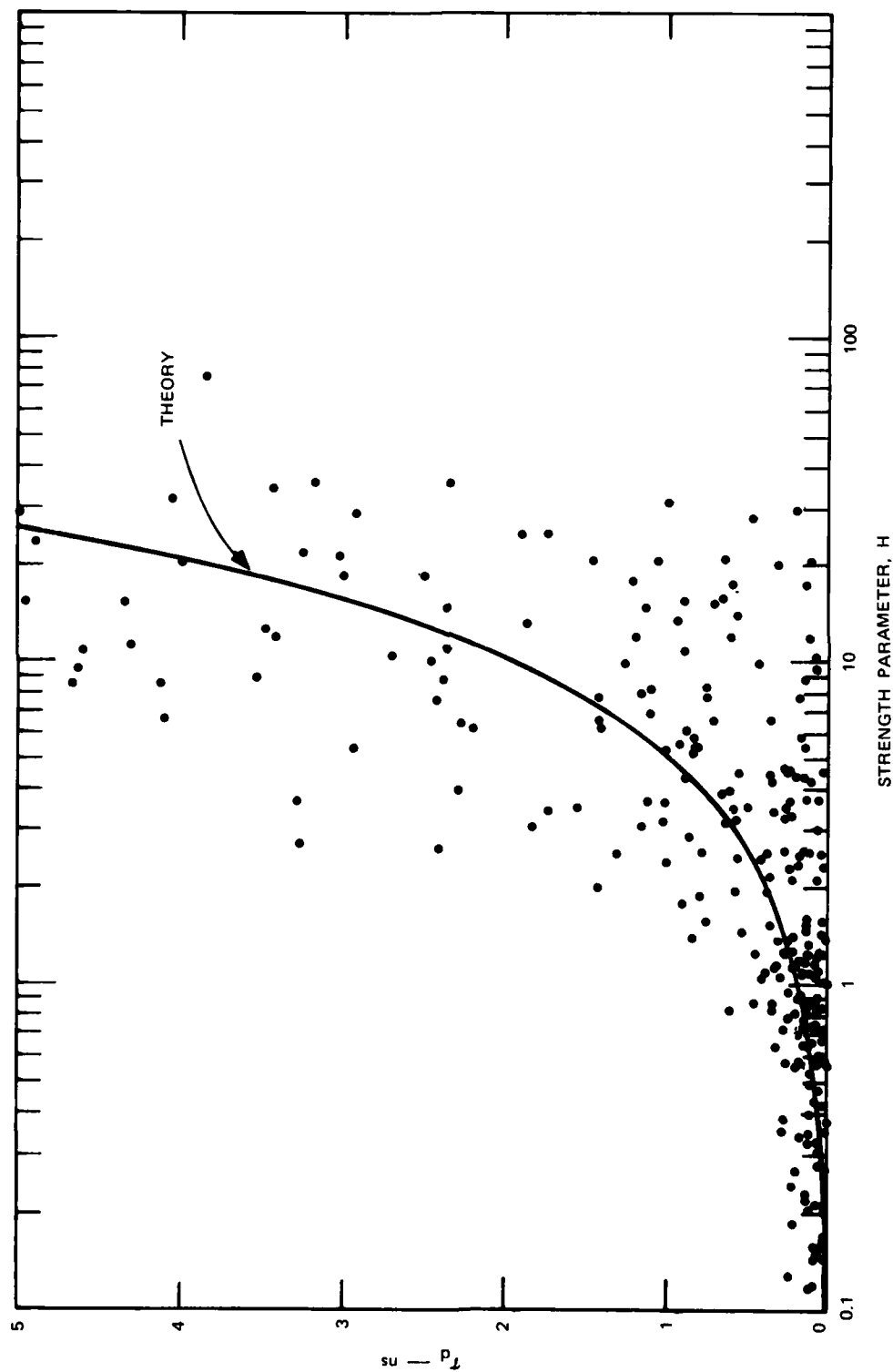


FIGURE 5 MEASUREMENTS OF DELAY JITTER FROM SYNTHESIZED PULSES USING WIDEBAND SATELLITE DATA TOGETHER WITH THEORETICAL PREDICTION FROM EQ. (IV-4)

V DISCUSSION

In this report we developed a theoretical model for computing the single-point, two-frequency coherence function that characterizes the ionospheric coherence bandwidth loss (Section II). We followed the method of Fante (1978), who proceeded from the Huygens-Fresnel principle and then used the Rytov approximation to determine the input conditions. In our approach we simplified the computation by neglecting the diffraction effects as predicted by the Rytov method, thereby assigning all the diffraction effects to free-space propagation.

As discussed in detail in Rino (1979a,b), this approach generally gives simple equivalent or "lumped" parameters that characterize the ionospheric perturbation and the resultant diffraction effects. Indeed, in the case of the shallowly sloped spectra ($\nu < 1.5$) that seem to characterize ionospheric irregularities, a single parameter H defined by Eq. (II-17) characterizes the combined effects of increased perturbation strength and propagation distance. The H parameter, like the U parameter that characterizes the corresponding effects in intensity scintillation data (Rino, 1979b), does not depend on the inner- or outer-scale cutoff wavenumbers.

The theory is in good agreement with measured frequency coherence functions using the Wideband satellite data (Section III). A crude approximation, Eq. (II-18), to the integral form of the theoretical model tends to underestimate the observed amount of frequency decorrelation, but gives acceptable results for engineering applications. In this regard, we also synthesized a pulse using the Wideband comb of seven equally spaced UHF transmissions and then measured the delay jitter. Moment estimates by their very nature produce large amounts of scatter, but good overall agreement between the measurements and the theory was obtained.

In a series of papers, Yeh and Liu have developed a detailed formalism for computing the signal moments that characterize the ionosphere-induced delay jitter and pulse smearing. Their method relies on a Taylor series expansion that suppresses the dependence of coherence bandwidth effects on the power-law index and depends on both the inner- and outer-scale cutoff wavenumbers. If the same (quadratic) approximation is used in our own model, Yeh and Liu's results can be recovered. For example, our formula for τ_d is equivalent to t_3 given by Eq. (5) in Yeh and Liu (1977).

To show the differences in the predicted values, in Figure 6 we have computed τ_d using both the small q_0 (asymptotic) and quadratic approximations for respective spectral indices in ranges where the approximations are valid. For the quadratic approximation, an outer scale of 10 km was used ($q_0/2\pi = 10$ km), and an inner scale of 100 m. The results were computed for a 1-GHz signal and plotted against C_s to facilitate comparisons with Figure 8 in Rino (1979a).

It can be seen that the quadratic theory predicts much smaller delay jitter than does the small q_0 asymptotic theory. These results are not in conflict, but illustrate the critical dependence of the theory on the power-law index. All the Wideband data that have been analyzed to date have favored the more shallowly sloped spectra where the asymptotic theory is valid. We have, moreover, recently found evidence that the spectral index varies with changing perturbation strength (Livingston and Rino, 1980). The effects of a varying spectral index are clearly evident in the frequency coherence data presented in Section III.

The theory developed in this report can be applied essentially over the full range of spectral indices that might occur in a disturbed nuclear environment. The simple formulas for the delay jitter and pulse broadening can be applied to get a rough estimate of the effects in precision navigation systems, for example. More refined calculations and/or simulations can be performed by using the full frequency coherence function.

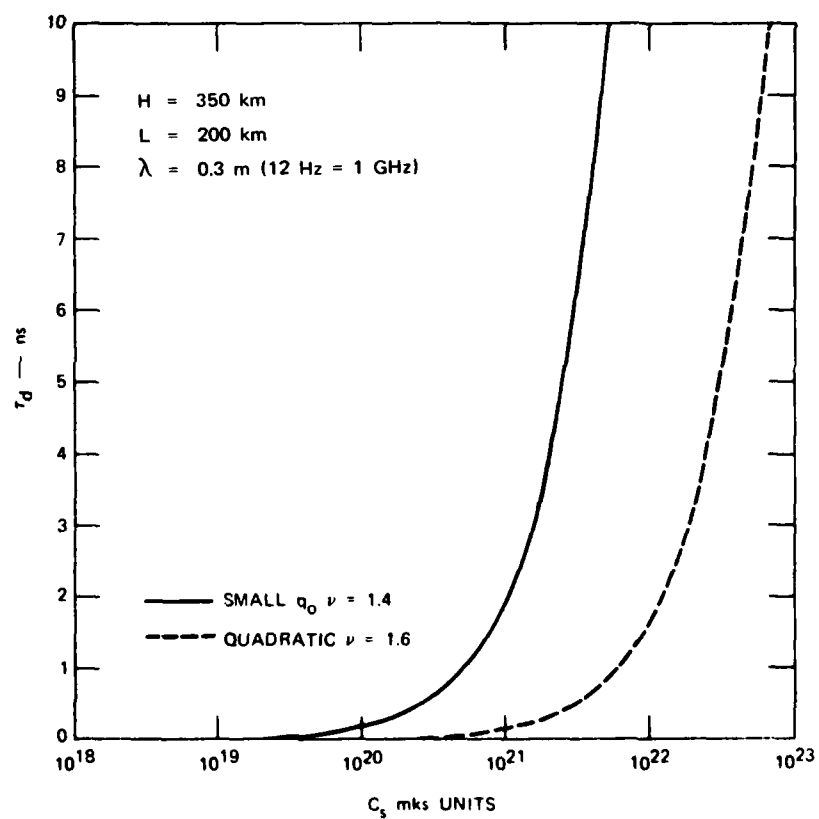


FIGURE 6 THEORETICAL CALCULATIONS OF DELAY JITTER CAUSED BY LOSS OF COHERENCE BANDWIDTH

REFERENCES

- Bello, P. A., "Characterization of Randomly Time-Variant Linear Channels," IEEE Trans. Comm. Systems., Vol. CS 11, p. 360, 1963.
- Fante, R. L., "Multiple-Frequency Mutual Coherence Functions for a Beam in a Random Medium," IEEE Trans. Ant. and Prop., Vol. AP-26, p. 621, 1978.
- Fremouw, E. J., R. L. Leadabrand, R. C. Livingston, M. D. Cousins, C. L. Rino, B. C. Fair, and R. A. Long, "Early Results from the DNA Wideband Satellite Experiment--Complex-Signal Scintillation," Radio Sci., Vol. 13, p. 167, 1978.
- Ishimaru, A., "Temporal Frequency Spectra of Multifrequency Waves in Turbulent Atmosphere," IEEE Trans. Ant. Prop., Vol. AP-20, p. 10, January 1972.
- Klobuchar, J. A., "A First Order, Worldwide, Ionospheric, Time-Delay Algorithm," AFCRL-TR-0502, NTIS AD A018862, September 25, 1975.
- Liu, C. H. and K. C. Yeh, "Statistics of Pulse Arrival Time in Turbulent Media," J. Opt. Soc. Am., Vol. 70, p. 168, February 1980.
- Liu, C. H. and K. C. Yeh, "Pulse Spreading and Wandering in Random Media," Radio Sci., Vol. 14, p. 925, 1979.
- Rino, C. L., "A Power-Law Phase Screen Model for Ionospheric Scintillation 1. Weak Scatter," Radio Sci., Vol. 14, p. 1135, 1979a.
- Rino, C. L., "A Power-Law Phase Screen Model for Ionospheric Scintillation 2. Strong Scatter," Radio Sci., Vol. 14, p. 1147, 1979b.
- Rino, C. L. and E. J. Fremouw, "The Angle Dependence of Singly Scattered Wavefields," J. Atmos. Terr. Phys., Vol. 39, p. 859, 1977.
- Rino, C. L. and J. Owen, "The Time Structure of Transionospheric Radio-wave Scintillation," Radio Sci., accepted for publication, 1980.
- Spilker, J. J., Jr., "GPS Signal Structure and Performance Characteristics," Navigation, Vol. 25, p. 121, Summer 1978.
- Yeh, K. C. and C. H. Liu, "Ionospheric Effects on Radio Communication and Ranging Pulses," IEEE Trans. Ant. and Prop., AP-27, p. 747, 1979.

Yeh, K. C. and C. H. Liu, "An Investigation of Temporal Moments of Stochastic Waves," Radio Sci., Vol. 12, p. 671, 1977a.

Yeh, K. C. and C. H. Liu, "Diagnostics of the Turbulent State of Ionospheric Plasma by Propagation Methods," Radio Sci., Vol. 12, p. 1031, 1977b.

Woo, R., "Multifrequency Techniques for Studying Interplanetary Scintillations," Astrophys. J., Vol. 201, p. 238, 1975.

Appendix

APPROXIMATIONS TO THE PHASE STRUCTURE FUNCTION

The general form of the phase structure function corresponding to the general power-law model summarized in Table 2 of Rino and Fremouw (1977) is

$$D_{\delta\phi}(q) = C_p \frac{\Gamma(\nu-1/2)}{2\pi\Gamma(\nu+1/2)} \left(\frac{\mathcal{L}(y)}{q_o^{2\nu-1}} \right) \quad (\text{A-1})$$

where

$$\mathcal{L}(y) = 1 - 2 \sqrt{r^2 + (q_o y/2)^2}^{\nu-1/2} K_{\nu-1/2} \left(2 \sqrt{r^2 + (q_o y/2)^2} \right) / N \quad (\text{A-2})$$

$$r = q_o/q_i \ll 1 \quad (\text{A-3})$$

and

$$N = \frac{1}{2} r^{\nu-1/2} K_{\nu-1/2}(2r) \cong \Gamma(\nu-1/2) \quad (\text{A-4})$$

A plot of $\mathcal{L}(y)$ is shown in Figure (A-1).

It was shown in Rino (1979b) that

$$\mathcal{L}(y) \sim C_{\delta\phi}^2 |y|^{2\nu-1} \quad (\text{A-5})$$

as long as $0.5 < \nu < 1.5$. The formal Taylor series expansion of Eq. (A-2) can be written

$$\mathcal{L}(y) = \sum_{k=1}^{\infty} D_n (q_o y)^{2n} \quad (\text{A-6})$$

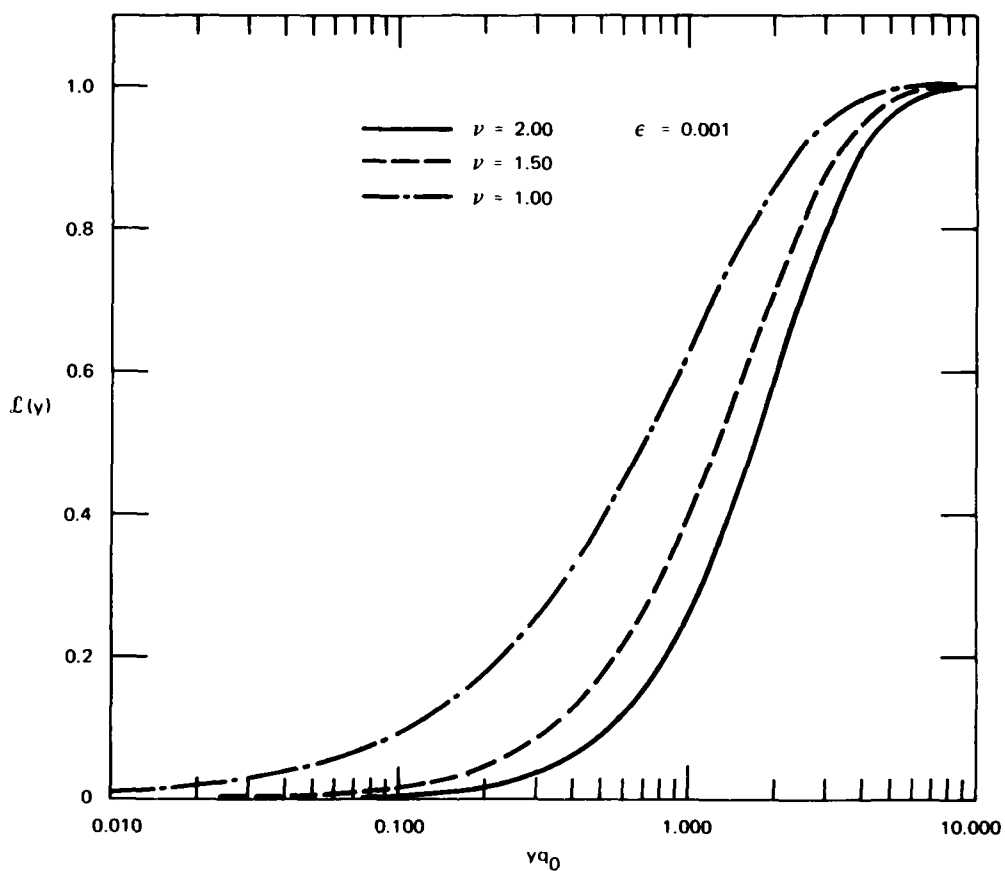


FIGURE A-1 PLOT OF NORMALIZED STRUCTURE FUNCTION SHOWING DEPENDENCE ON SPECTRAL SLOPE

where

$$D_n = \frac{\partial^{2n} \mathcal{L}(y)}{(2n)! \partial y^{2n}} \bigg|_{y=0} \quad (A-7)$$

For our purposes here we need only consider the first nonzero coefficient

$$D_1 = \frac{1}{2} r^{\nu-3/2} K_{\nu-3/2}(2\epsilon)/N$$

$$\approx \begin{cases} -\frac{1}{2} \log(2r) & \nu = 1/5 \\ \frac{\Gamma(\nu-1.5)}{4\Gamma(\nu-0.5)} & \nu > 1.5 \end{cases} \quad (A-8)$$

Higher-order coefficients become increasingly more sensitive to the inner-scale cutoff.

In Figure (A-2) the small q_0 approximation is shown on an expanded plot of the exact form of $f(y)$. In Figure (A-3) the corresponding plot for the quadratic approximation is shown. The asymptotic approximation is applicable when $\nu < 1.4$ and improves as ν decreases, whereas the quadratic approximation applies when $\nu > 1.5$ and improves with increasing ν . Both approximations are, of course, only valid for $q_0 y \ll (2\pi)^{-1}$. Because of the very large outer-scale wavelength that characterizes ionospheric irregularities, however, this is generally a very good approximation.

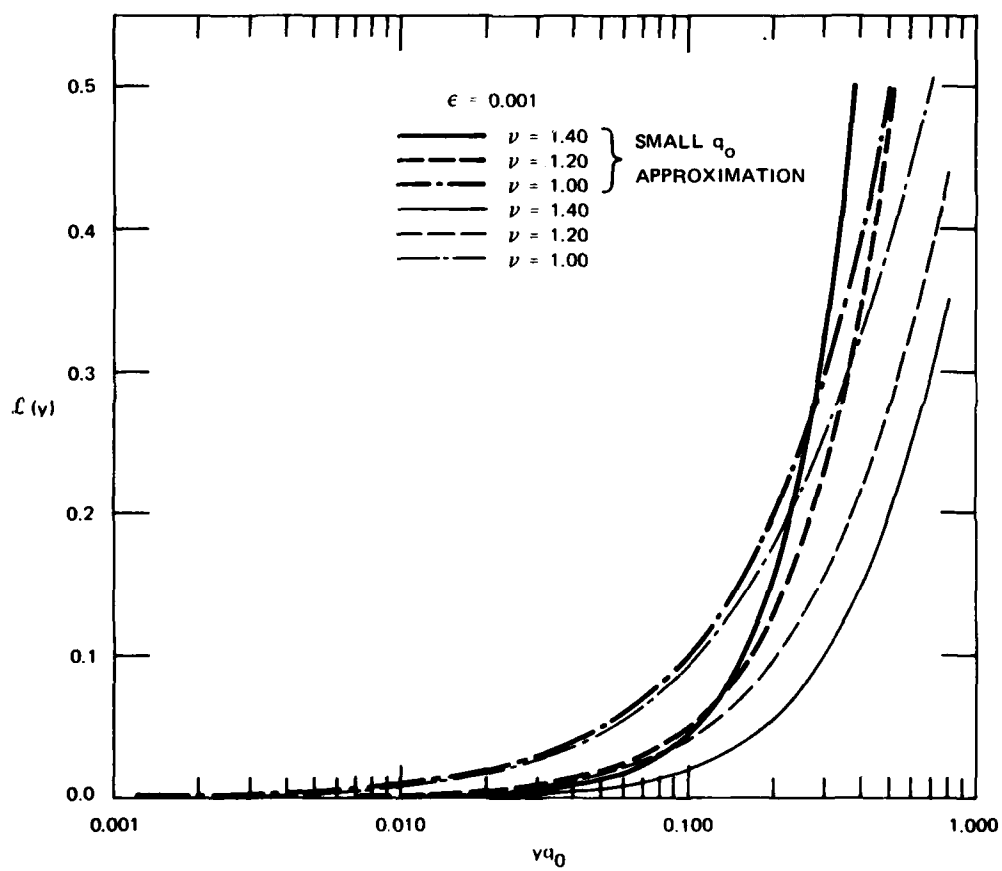


FIGURE A-2 PLOT OF SMALL q_0 APPROXIMATION TO PHASE STRUCTURE FUNCTION (valid for $\nu < 1.5$) SUPERIMPOSED ON EXACT CURVES

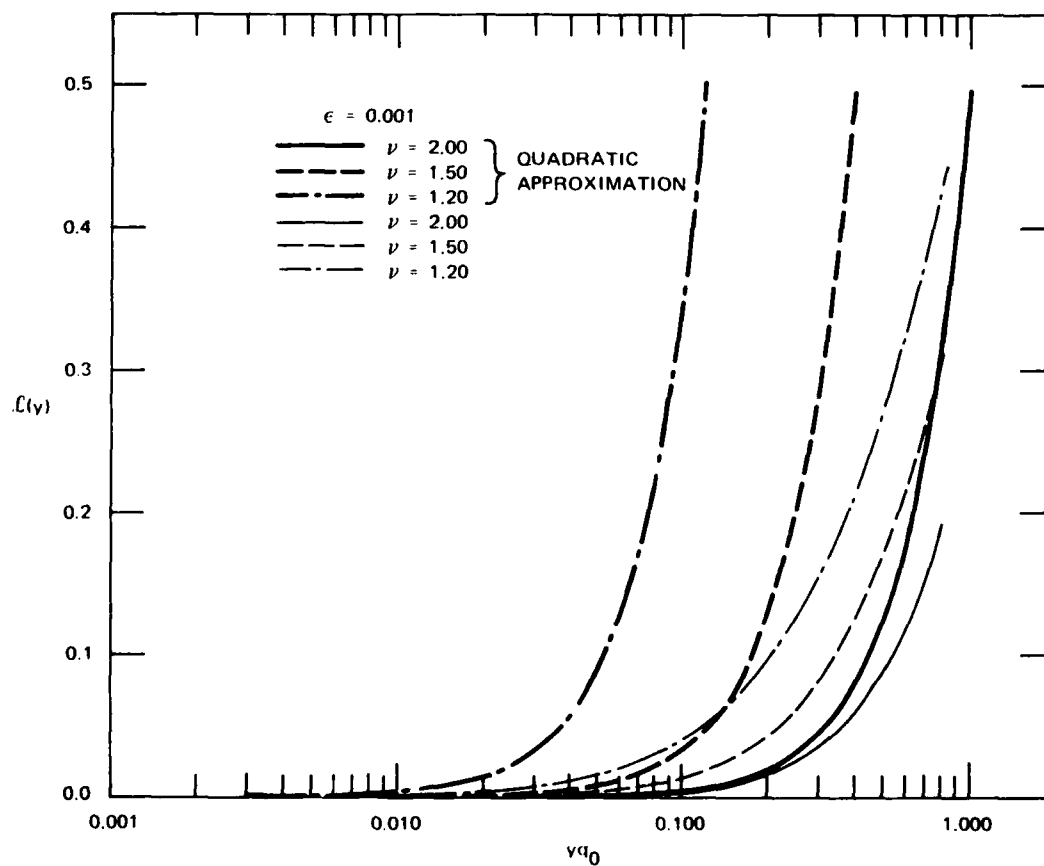


FIGURE A-3 PLOT OF QUADRATIC APPROXIMATION TO PHASE STRUCTURE FUNCTION SUPERIMPOSED ON EXACT CURVES

DISTRIBUTION LIST

DEPARTMENT OF DEFENSE

Assistant Secretary of Defense
Comm, Cmd, Cont & Intell
ATTN: Dir of Intell Systems, J. Babcock
ATTN: C31st& CCS, M. Epstein

Assistant to the Secretary of Defense
Atomic Energy
ATTN: Executive Assistant

Command & Control Technical Center
Department of Defense
ATTN: C-312, R. Mason
ATTN: C-650, G. Jones
3 cy ATTN: C-650, W. Heidig

Defense Advanced Rsch Proj Agency
ATTN: TIO

Defense Communications Agency
ATTN: Code 480, F. Dieter
ATTN: Code 1018
ATTN: Code 810, J. Barna
ATTN: Code 480
ATTN: Code 205

Defense Communications Engineer Center
ATTN: Code R720, J. Worthington
ATTN: Code R123
ATTN: Code R410, J. McLean
ATTN: Code R410, R. Craighill

Defense Intelligence Agency
ATTN: DT-5
ATTN: DB-4C, E. O'Farrell
ATTN: DB, A. Wise
ATTN: DT-1B
ATTN: HQ-TR, J. Stewart
ATTN: DC-7D, W. Wittig

Defense Nuclear Agency
ATTN: STNA
3 cy ATTN: RAAE
4 cy ATTN: TITL

Defense Technical Information Center
12 cy ATTN: DD

Field Command
Defense Nuclear Agency
ATTN: FCPR

Field Command
Defense Nuclear Agency
Livermore Division
ATTN: FCPRL

Interservice Nuclear Weapons School
ATTN: TTV

Joint Chiefs of Staff
ATTN: C3S
ATTN: C3S, Evaluation Office

DEPARTMENT OF DEFENSE (Continued)

Joint Strat Tgt Planning Staff
ATTN: JLA
ATTN: JLTW-2

National Security Agency
ATTN: B-3, F. Leonard
ATTN: R-52, J. Skillman
ATTN: W-32, O. Bartlett

Undersecretary of Def for Rsch & Engr
Department of Defense
ATTN: Defensive Systems
ATTN: Strategic & Space Systems (OS)

WWMCCS System Engineering Org
ATTN: R. Crawford

DEPARTMENT OF THE ARMY

ACofS for Automation & Comm
Department of the Army
ATTN: DAAC-ZT, P. Kenny

Atmospheric Sciences Lab
U.S. Army Electronics R&D Command
ATTN: DELAS-AS, H. Holt
ATTN: DELAS-EO, F. Niles

BMD Advanced Technology Center
Department of the Army
ATTN: ATC-T, M. Capps
ATTN: ATC-O, W. Davies
ATTN: ATC-R, D. Russ

BMD Systems Command
Department of the Army
2 cy ATTN: BMDSC-HW

Deputy chief of Staff for Ops & Plans
Department of the Army
ATTN: DAMO-RQC

Electronics Tech & Devices Lab
U.S. Army Electronics R&D Command
ATTN: DELET-ER, H. Bomke

Harry Diamond Labs
Department of the Army
ATTN: DELHD-N-RB, R. Williams
ATTN: DELHD-N-P
ATTN: DELHD-N-P, F. Wimenitz
ATTN: DELDH-I-TL
ATTN: DELHD-I-TL, M. Weiner

U.S. Army Comm-Elec Engrg Instal Agency
ATTN: CCC-CED-CCO, W. Neuendorf
ATTN: CCC-EMEO-PED, G. Lane
ATTN: CCC-EMEO, W. Nair

U.S. Army Communications Command
ATTN: CC-OPS-WR, H. Wilson
ATTN: CC-OPS-W

DEPARTMENT OF THE ARMY (Continued)

U.S. Army Communications R&D Command
ATTN: DRDCO-COM-RY, W. Kesselman

U.S. Army Foreign Science & Tech Ctr
ATTN: DRXST-SD

U.S. Army Materiel Dev & Readiness Cmd
ATTN: DRCLDC, J. Bender

U.S. Army Missile Command
2 cy ATTN: Redstone Scientific Info Ctr

U.S. Army Missile Intelligence Agency
ATTN: J. Gamble

U.S. Army Nuclear & Chemical Agency
ATTN: Library

U.S. Army Satellite Comm Agency
ATTN: Document Control

U.S. Army Tradoc Systems Analysis Act
ATTN: ATAA-TDC
ATTN: ATAA-PL
ATTN: ATAA-TCC, F. Payan, Jr

DEPARTMENT OF THE NAVY

Joint Cruise Missiles Project
Department of the Navy
ATTN: JCMG-707

Naval Air Development Center
ATTN: Code 6091, M. Setz

Naval Air Systems Command
ATTN: PMA 271

Naval Electronic Systems Command
ATTN: Code 3101, T. Hughes
ATTN: Code 501A
ATTN: PME 106-13, T. Griffin
ATTN: PME 106-4, S. Kearney
ATTN: PME 117-20
ATTN: PME 117-211, B. Kruger
ATTN: PME 117-2013, G. Burnhart

Naval Intelligence Support Ctr
ATTN: NISC-50

Naval Ocean Systems Center
ATTN: Code 532, J. Bickel
ATTN: Code 5322, M. Paulson
3 cy ATTN: Code 5324, W. Moler

Naval Research Laboratory
ATTN: Code 7500, B. Wald
ATTN: Code 4700, T. Coffey
ATTN: Code 4780, S. Ossakow
ATTN: Code 2627
ATTN: Code 5300
ATTN: Code 7550, J. Davis
ATTN: Code 4701, J. Brown
ATTN: Code 6730, E. McClean

Naval Space Surveillance System
ATTN: J. Burton

DEPARTMENT OF THE NAVY (Continued)

Naval Surface Weapons Center
ATTN: Code F31

Naval Surface Weapons Center
ATTN: Code F-14, R. Butler

Naval Telecommunications Command
ATTN: Code 341

Office of Naval Research
ATTN: Code 465
ATTN: Code 421
ATTN: Code 420

Office of the Chief of Naval Operations
ATTN: OP 65
ATTN: OP 981N
ATTN: OP 941D

Strategic Systems Project Office
Department of the Navy
ATTN: NSP-2141
ATTN: NSP-43
ATTN: NSP-2722, F. Wimberly

DEPARTMENT OF THE AIR FORCE

Aerospace Defense Command
ATTN: DC, T. Long

Air Force Geophysics Lab
ATTN: OPR-1, J. Ulwick
ATTN: PHP, J. Aarons
ATTN: LKB, K. Champion
ATTN: OPR, A. Stair
ATTN: OPR, H. Gardiner
ATTN: PHI, J. Euchau
ATTN: PHP, J. Mullen

Air Force Weapons Lab
Air Force Systems Command
ATTN: SUL
ATTN: DYC
ATTN: CA

Air Force Wright Aeronautical Labs
ATTN: AAD, W. Hunt
ATTN: A. Johnson

Air Logistics Command
Department of the Air Force
ATTN: OO-ALC/MM, R. Blackburn

Assistant Chief of Staff
Intelligence
Department of the Air Force
ATTN: INED

Assistant Chief of Staff
Studies and Analyses
Department of the Air Force
ATTN: AF/SASC, G. Zank
ATTN: AF/SASC, W. Adams

Electronic Systems Division
ATTN: DCKC, J. Clark

DEPARTMENT OF THE AIR FORCE (Continued)

Ballistic Missile Office
Air Force Systems Command
ATTN: MNNL, S. Kennedy
ATTN: MNX
ATTN: MNNL
ATTN: MNNH
ATTN: MNNH, M. Baran

Operations Plans and Readiness
Department of the Air Force
ATTN: AFXOKS
ATTN: AFXOXFD
ATTN: AFXOKT
ATTN: AFXOKCD

Research, Development & Acq
Department of the Air Force
ATTN: AFRDSP
ATTN: AFRDQ
ATTN: AFRDS
ATTN: AFRDSS

Electronic Systems Division
ATTN: XRW, J. Deas

Electronic Systems Division
ATTN: YSEA
ATTN: YSM, J. Kobelski

Foreign Technology Division
Air Force Systems Command
ATTN: NIIS Library
ATTN: SDEC, A. Oakes
ATTN: TQTD, B. Ballard

Headquarters Space Division
Air Force Systems Command
ATTN: RSP

Headquarters Space Division
Air Force Systems Command
ATTN: SKA, M. Clavin
ATTN: SKA, C. Rightmyer

Headquarters Space Division
Air Force Systems Command
ATTN: SZJ
ATTN: SZJ, L. Doan
ATTN: SZJ, W. Mercer

Headquarters Space Division/YA
Air Force Systems Command
ATTN: E. Butt

Rome Air Development Center
Air Force Systems Command
ATTN: OCS, V. Coyne
ATTN: TSLD

Strategic Air Command
Department of the Air Force
ATTN: XPFS, B. Stephan
ATTN: DCXF
ATTN: OOKSN
ATTN: XPFS
ATTN: DCXT
ATTN: NRT
ATTN: ADWATE, B. Bauer
ATTN: DCXT, T. Jorgensen
ATTN: DCX

DEPARTMENT OF THE AIR FORCE (Continued)

Rome Air Development Center
Air Force Systems Command
ATTN: EEP

DEPARTMENT OF ENERGY CONTRACTORS

EG&G, Inc
Los Alamos Division
ATTN: D. Wright
ATTN: J. Colvin

Lawrence Livermore National Lab
ATTN: L-389, R. Ott
ATTN: L-31, R. Hager
ATTN: L-96, T. Donich
ATTN: Technical Info Dept Library

Los Alamos National Scientific Lab
ATTN: MS664, J. Zinn
ATTN: MS670, J. Hopkins
ATTN: P. Keaton
ATTN: D. Simons
ATTN: MS668, J. Malik
ATTN: E. Jones
ATTN: D. Westervelt
ATTN: R. Taschek

Sandia National Laboratories
Livermore Laboratory
ATTN: B. Murphey
ATTN: T. Cook

Sandia National Laboratories
ATTN: D. Thornbrough
ATTN: 3141
ATTN: Org 1250, W. Brown
ATTN: C. Williams
ATTN: Space Project Div
ATTN: D. Dahlgren
ATTN: C. Mehl
ATTN: Org 4241, T. Wright

OTHER GOVERNMENT AGENCIES

Central Intelligence Agency
ATTN: OSWR/NED

Department of Commerce
National Bureau of Standards
ATTN: R. Moore

Department of Commerce
National Oceanic & Atmospheric Admin
Environmental Research Labs
ATTN: D. Williams
ATTN: R. Grubb

Institute for Telecommunications Sciences
National Telecommunications & Info Admin
ATTN: D. Crombie
ATTN: W. Utlaut
ATTN: A. Jean
ATTN: L. Berry

U.S. Coast Guard
Department of Transportation
ATTN: G-DOE-3/TP54, B. Romine

DEPARTMENT OF DEFENSE CONTRACTORS

Aerospace Corp

ATTN: R. Slaughter
ATTN: A. Morse
ATTN: S. Bower
ATTN: V. Josephson
ATTN: T. Salmi
ATTN: W. Grabowsky
ATTN: G. Anderson
ATTN: F. Morse
ATTN: I. Garfunkel
ATTN: N. Stockwell
ATTN: D. Olsen

Analytical Systems Engineering Corp
ATTN: Radio Sciences

Analytical Systems Engineering Corp
ATTN: Security

APTEK

ATTN: T. Meagher

Barry Research Corp

ATTN: J. McLaughlin

BDM Corp

ATTN: T. Neighbors
ATTN: L. Jacobs

Berkeley Research Associates, Inc

ATTN: J. Workman

Boeing Company

ATTN: M/S 42-33, J. Kennedy
ATTN: G. Hall
ATTN: S. Tashird

Univ of California at San Diego
Electrical Engineering Computer Sciences
ATTN: H. Booker

Charles Stark Draper Lab, Inc

ATTN: J. Gilmore
ATTN: D. Cox

Computer Sciences Corp

ATTN: H. Blank

Comsat Labs

ATTN: G. Hyde
ATTN: R. Taur

Cornell University

Department of Electrical Engineering
ATTN: D. Farley, Jr

University of Alaska

Geophysical Institute
ATTN: N. Brown
ATTN: T. Davis
ATTN: Technical Library

Electrospace Systems, Inc

ATTN: P. Phillips
ATTN: H. Logston

ESL, Inc

ATTN: J. Marshall

DEPARTMENT OF DEFENSE CONTRACTORS (Continued)

Ford Aerospace & Communications Corp

ATTN: J. Mattingley

General Electric Co

Space Division

ATTN: R. Edsall
ATTN: M. Bortner
ATTN: A. Harcar

General Electric Co

Re-Entry & Environmental Systems Div

ATTN: A. Steinmayer
ATTN: C. Zierdt

General Electric Co

ATTN: F. Reibert
ATTN: G. Millman

General Electric Company—TEMPO

ATTN: M. Stanton
ATTN: W. Knapp
ATTN: T. Stevens
ATTN: D. Chandler
ATTN: DASIAC
ATTN: W. McNamara

General Electric Tech Srv Co, Inc

ATTN: G. Millman

General Research Corp

ATTN: J. Ise, Jr
ATTN: J. Garbarino

Sylvania Systems Group

ATTN: M. Cross

HSS, Inc

ATTN: D. Hansen

IBM Corp

ATTN: F. Ricci

University of Illinois

ATTN: K. Yeh

Information Science, Inc

ATTN: W. Dudziak

Institute for Defense Analyses

ATTN: J. Aein
ATTN: J. Bengston
ATTN: H. Wolfhard
ATTN: E. Bauer

International Tel & Telegraph Corp

ATTN: G. Wetmore
ATTN: Technical Library

JAYCOR

ATTN: S. Goldman

JAYCOR

ATTN: D. Carlos

Kaman Sciences Corp

ATTN: N. Beauchamp
ATTN: F. Foxwell

DEPARTMENT OF DEFENSE CONTRACTORS (Continued)

Johns Hopkins University
Applied Physics Lab
ATTN: P. Komiske
ATTN: T. Potemra
ATTN: T. Evans
ATTN: J. Newland
ATTN: B. Wise

Linkabit Corp
ATTN: I. Jacobs

Litton Systems, Inc
ATTN: R. Grasty

Lockheed Missiles & Space Co, Inc
ATTN: W. Imhof
ATTN: M. Walt
ATTN: R. Johnson
ATTN: R. Au

Lockheed Missiles & Space Co, Inc
ATTN: Dept 60-12
ATTN: D. Churchill

M.I.T. Lincoln Lab
ATTN: D. Towle
ATTN: L. Loughlin
ATTN: J. Evans

Martin Marietta Corp
ATTN: R. Heffner

McDonnell Douglas Corp
ATTN: J. Moule
ATTN: G. Mroz
ATTN: W. Olson
ATTN: R. Halprin
ATTN: N. Harris

Meteor Communications Consultants
ATTN: R. Leader

Mission Research Corp
ATTN: D. Sowle
ATTN: C. Longmire
ATTN: S. Gutsche
ATTN: F. Fajen
ATTN: R. Hendrick
ATTN: R. Bogusch
ATTN: M. Scheibe
ATTN: D. Sappenfield
ATTN: R. Kilb

Mitre Corp
ATTN: B. Adams
ATTN: G. Harding
ATTN: A. Kymmel
ATTN: C. Callahan

Mitre Corp
ATTN: W. Hall
ATTN: W. Foster
ATTN: M. Horrocks
ATTN: J. Wheeler

Pacific-Stierra Research Corp
ATTN: E. Field, Jr
ATTN: F. Thomas

DEPARTMENT OF DEFENSE CONTRACTORS (Continued)

Pennsylvania State University
ATTN: Ionospheric Research Lab

Photometrics, Inc
ATTN: I. Kofsky

Physical Dynamics, Inc
ATTN: E. Fremouw

R & D Associates
ATTN: W. Wright, Jr
ATTN: R. Turco
ATTN: F. Gilmore
ATTN: C. MacDonald
ATTN: W. Karzas
ATTN: C. Greifinger
ATTN: H. Ory
ATTN: R. Lelevier
ATTN: M. Gantsweg
ATTN: B. Gabbard
ATTN: P. Haas

R & D Associates
ATTN: B. Yoon
ATTN: L. Delaney

Rand Corp
ATTN: C. Crain
ATTN: E. Bedrozian

Raytheon Company
ATTN: G. Thone

Riverside Research Institute
ATTN: V. Trapani

Rockwell International Corp
ATTN: J. Kristof

Sante Fe Corp
ATTN: D. Paolucci

Science Applications, Inc
ATTN: D. Sachs
ATTN: D. Hamlin
ATTN: E. Straker
ATTN: L. Linson
ATTN: R. Lee
ATTN: J. McDougall
ATTN: C. Smith

Science Applications, Inc
ATTN: SZ

Science Applications, Inc
ATTN: J. Cockayne

SRI International
ATTN: A. Burns
ATTN: R. Livingston
ATTN: M. Baron
ATTN: R. Leonard
ATTN: R. Leadaerand
ATTN: W. Chesnut
ATTN: G. Price
ATTN: G. Smith
ATTN: D. Neilson
ATTN: J. Depp
ATTN: C. Rino
ATTN: W. Jaye

DEPARTMENT OF DEFENSE CONTRACTORS (Continued)

SRI International
ATTN: F. Perkins

Technology International Corp
ATTN: W. Boquist

TeleDyne Brown Engineering
ATTN: N. Passino

TRW Defense & Space Sys Group
ATTN: D. Dee
ATTN: R. Plebuch
ATTN: S. Altschuler

DEPARTMENT OF DEFENSE CONTRACTORS (Continued)

Tri-Com, Inc
ATTN: D. Murray

Utah State University
Space Measurements Lab
ATTN: K. Baker
ATTN: J. Dupnik
ATTN: L. Jensen

VisiDyne, Inc
ATTN: C. Humphrey
ATTN: J. Carpenter